Theor Chem Acc (2016) 135:229
DOI 10.1007/s00214-016-1986-6

REGULAR ARTICLE

The influence of π-conjugation framework on intramolecular proton transfer and Stokes shift in 1,8-Dihydroxydibenzo[a,c] phenazine molecule: a DFT and TD-DFT study

Chi Ma[1] · Yonggang Yang[1] · Chaozheng Li[1] · Yufang Liu[1]

Received: 14 April 2016 / Accepted: 13 August 2016 / Published online: 25 August 2016

Abstract The 1,8-Dihydroxydibenzo[a,c]phenazine (DHBP) is chosen to investigate the relationship among the extension of π-conjugation framework, excited-state proton transfer and the Stokes shift. The IR spectra, bond and angle analyses show that the two intramolecular hydrogen bonds in DHBP molecule are both significantly strengthened in S_1 state. The proton donor methanol molecule can inhibits the hydrogen bond strengthening in S_1 state. The increment of π-conjugation framework effectively decreases the Stokes shift and promotes the proton transfer. The potential energy surfaces of DHBP indicate that the reverse double-proton transfer can spontaneously happen in S_0 state, and the double proton can easily transfer for its relative low potential energy barrier in S_1 state.

Keywords ESDPT · IR and electronic spectra · Potential energy surface · The Stokes shift · NBO charges

1 Introduction

Excited-state proton transfer (ESPT) refers to proton(s) migration induced by photo-excitation combined with drastic structural change and electron redistribution, which will provide unique fluorescence emission and large Stokes shift. These characters make the ESPT molecule been widely used in many physical and biological systems, such as fluorescence sensors [1], laser dyes [2], UV filters [3], molecular switches [4] and LEDs [5]. Recent developments in chemistry and physics have heightened the need for clear and comprehensive explanation of excited-state proton transfer mechanism [6–8] and the influence factors on Stokes shift [9, 10]. A vast number of attempts have been made since the excited-state proton transfer (ESPT) phenomenon was first observed in the characteristic experiment with methyl salicylate by Weller and co-workers [11]. Taylor et al. [12] found that the 7-azaindole dimer has different tautomer in ground and first excited states, which is the first recorded example of concerted biprotonic transfer. Martinez et al. [13] proposed that the strong bathochromic fluorescence shift of 10-hydroxybenzo-[h]quinoline (HBQ) can be explained by ESIPT process. Lischka et al. [14] concluded a sequential proton transfer mechanism after carefully investigating the double-proton transfer reaction in [2,20-bipyridyl]-3,-30-diol. Then, the potential energy surface was used to investigate the double-proton transfer process of 7-azaindole dimer system by Ando et al. [15] It was not until the end of the 20th century that people began to realize the fundamental role of weak interaction in proton transfer process [16, 17]. The hydrogen bond, as one of the most important weak interactions, has attracted great attention [18–21] owing to its directional character in many photo-physical and photo-chemical reactions, especially in the excited-state intra- and intermolecular proton transfer process. In an investigation into excited-state hydrogen bond, Han et al. [22, 23] found the intermolecular hydrogen bond strengthening phenomenon after photo-excitation. Recently, the DFT and TDDFT methods were used by Zhao et al. [24] to optimize the phenol-borane-trimethylamine complex in ground and electronically excited states, and they found that the excited-state hydrogen bond strengthening can facilitate the proton transfer process

Electronic supplementary material The online version of this article (doi:10.1007/s00214-016-1986-6) contains supplementary material, which is available to authorized users.

✉ Yufang Liu
yf-liu@htu.cn

[1] College of Physics and Material Science, Henan Normal University, Xinxiang 453007, China

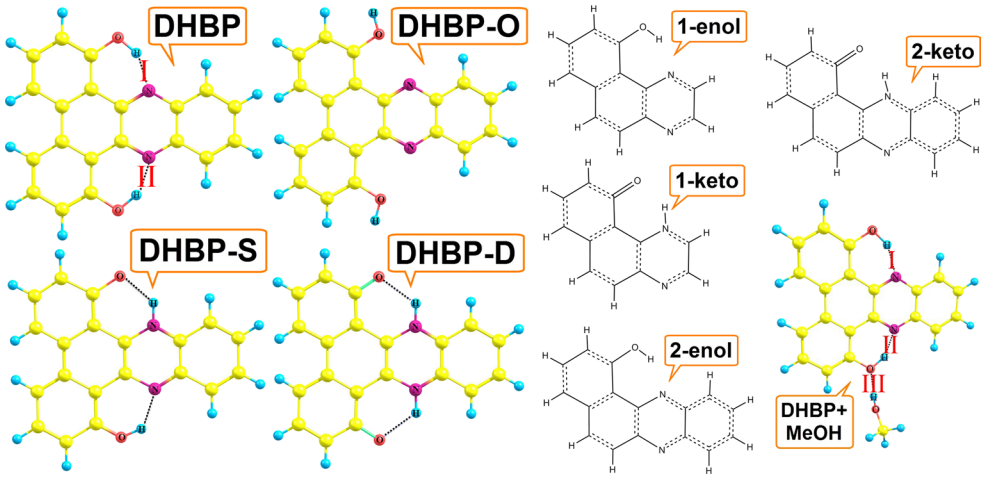

Fig. 1 Configuration 1 and 2; optimized structures of DHBP, DHBP-O (open), DHBP-S (single), DHBP-D (double) and DHBP+MeOH in ground state

effectively. Through analyzing the potential energy surface of 3-hydroxyisoquinoline (3HIQ), which is calculated in the same methods, a new double-proton transfer mechanism was clearly proposed by Zhao et al. [25]. Although extensive researches have been carried out on proton transfer process, few investigators have been able to draw on any systematic research into excited-state proton transfer mechanism and the influence factors on Stokes shift. Recently, the 1,8-Dihydroxydibenzo[a,c]phenazine (DHBP) that contains two intramolecular hydrogen bonds was demonstrated experimentally by Piechowska et al. [26]. In their seminal study, compared with the corresponding 10-hydroxybenzo[h]quinoline, the emission spectrum of the π-expanded phenazine analogues was weaker but displayed a characteristic bathochromic shift into NIR region. In the present work, the excited-state intramolecular proton transfer mechanism and the influence factors on Stokes shift were mainly proposed. Due to the sufficient accuracy of DFT and TDDFT methods proved in the previous studies [22–25], the DHBP molecule and its derivatives were optimized throughout this work with DFT and TDDFT methods. The configurations 1 and 2 (as shown in Fig. 1) are setting for comparison to investigate the influence of π-conjugation framework. The DHBP-O molecule was adjusted with hydroxyl groups rotated to avoid the formation of intramolecular hydrogen bonds. The IR spectral shifts were monitored to predict the changes of intramolecular hydrogen bonds. The electronic spectra, frontier molecular orbitals, NBO charges [27–30] and potential energy surfaces also been presented.

2 Computational details

In this work, all the electronic structure optimizations were performed using the Gaussian 09 program [31] package at the popular Becke's three-parameter hybrid exchange functional with Lee–Yang–Parr gradient-corrected correlation (B3LYP) [32–35] in ground state and long-rang corrected B3LYP (CAM)-B3LYP [36–38] in excited-states with the standard 6-31++G(d,p) level. Several functionals have been tested in this work, among them, the B3LYP and CAM-B3LYP can provide relative accurate results within a shorter machine hour. Some previous investigations on ESPT [19–21, 23–25] also confirm the sufficient flexibility of B3LYP and (CAM)-B3LYP functionals with 6-31++G(d,p) level. In order to be consistent with the previous experiment, toluene was chosen as the solvent based on the integral equation formalism variant of the polarizable continuum model (IEFPCM) [39–41]. The ground state configurations were fully optimized without any constraint of bonds, angles and dihedral angles. The vertical excitation energies were calculated by TDDFT method with IEFPCM based on ground state optimized structures. The theoretical calculation provided six low-lying absorbing transitions and the S_1 state geometries were optimized without constraint on the strength of the ground state equilibrium geometries. All the local minima geometries were confirmed without any imaginary modes in the vibrational analysis and calculation. Meanwhile, the potential energy surfaces were scanned in both S_0 and S_1 states with a series of fixed O_{23}–H_{24} and O_{25}–H_{26} bond lengths in constrained optimizations and frequency analyses. Harmonic vibrational frequencies in S_0 and S_1 states were determined by diagonalization of the Hessian. The excited-state Hessian was obtained by numerical differentiation of the analytical gradients using central differences and default displacements of 0.02 Bohr [42]. The infrared intensities were determined by the gradients of the dipole moment [43].

3 Results and discussion

3.1 The optimized geometric structures and infrared spectra

In the present work, the intramolecular hydrogen bonds were numerically labeled with I, II and III for better description. From Table 1, it is easy to note that the $(O–H)_I$ and $(O–H)_{II}$ both lengthen from 0.968 Å (S_0) in DHBP-O to 0.997 Å (S_0) in DHBP, indicating that the double intramolecular hydrogen bonds have been formed in DHBP molecule in ground state. After photo-excitation, in DHBP molecule, the hydroxyl groups both lengthen to 1.042 Å and the bond angles $\delta_{(O–H\cdots N)I,\ II}$ change from 148.0° (S_0) to 151.4° (S_1). The intramolecular hydrogen bonds I and II also clearly shorten to 1.545 Å (S_1), which could be conceivably concluded that the intramolecular hydrogen bonds I and II in DHBP are both strengthened after photo-excitation. For DHBP-S molecule, the bond length $(O\cdots H)_I$ changes from 1.575 Å (S_0) to 1.669 Å (S_1) and the bond angle $\delta_{(O\cdots H–N)I}$ changes from 145.1° (S_0) to 141.7° (S_1), indicating that the intramolecular hydrogen bond I is weakened in S_1 state. The bond length of $(H_{\cdots}N)_{II}$ changes from 1.708 Å (S_0) to 1.671 Å (S_1) and the $\delta_{(O–H\cdots N)II}$ changes from 148.1° (S_0) to 150.2° (S_1), implying that the intramolecular hydrogen bond II is strengthened after photo-excitation. The energy of the double intramolecular hydrogen bonds in DHBP molecule is 26.89 kcal/mol in ground state and 36.81 kcal/mol in first excited state, which further confirm the hydrogen bond strengthening phenomenon in S_1 state. Moreover, one methanol molecule was added to investigate the influence proton donor molecule. The intermolecular hydrogen bond III, which is formed between DHBP and methanol molecule, slightly weaken from 1.912 Å (S_0) to 1.902 Å (S_1). The intramolecular hydrogen bond I changes from 1.663 Å (S_0) to 1.479 Å (S_1) and that in position II has a slighter change from 1.633 Å (S_0) to 1.518 Å (S_1). The clear comparison indicates that the addition of methanol may inhibit the hydrogen bond strengthening after photo-excitation. In order to set a quite spectacular contrast, the configuration 1 and 2, which contain different number of benzene ring, were cut out from DHBP molecule. As is shown, the intramolecular hydrogen bonds are 1.725 Å (C1) and 1.709 Å (C2) in ground state. Compared with that in DHBP molecule (1.668 Å), the intramolecular hydrogen bond has visibly strengthened with the increment of π-conjugation framework. Due to the vibrational modes of functional groups involved in the hydrogen bonds are closely related to the hydrogen bond strengthening and weakening, the calculated O–H stretching vibration spectra of configuration 1, 2, DHBP and DHBP+MeOH in S_0 and S_1 states are presented in the Supporting Information. The vibrational peaks of hydroxyl groups in DHBP molecule are both located at 3126 cm^{-1} (S_0) and 2414 cm^{-1} (S_1). The large redshift suggests that the intramolecular hydrogen bonds are both strengthened after photo-excitation. Moreover, that in configuration 1 and 2 are located on 3233 cm^{-1} (S_0) and 3177 cm^{-1} (S_0), respectively. It is clearly seen that the vibrational spectra redshift with the increment of π-conjugation framework, which further confirm the conclusion we got above. The participation of methanol molecule makes the spectra have different changes in the same molecule, which redshift from 3093 cm^{-1} (S_0) to 2056 cm^{-1} (S_1) in position I and much weaker redshift from 2960 cm^{-1} (S_0) to 2252 cm^{-1} (S_1) in position II. The notable comparison indicates that the methanol molecule can inhibits the hydrogen bond strengthening in S_1 state.x

Table 1 Calculated bond lengths (Å) and angles (°) in ground and first excited state, respectively

	$(O–H)_I$	$(N\cdots H)_I$	$(O–H)_{II}$	$(N\cdots H)_{II}$	$\delta_{(O–H-N)I}$	$\delta_{(O–H-N)II}$	$(N\cdots H)_{III}$
DHBP							
S_0	0.999	1.668	0.999	1.668	148.06	148.02	
S_1	1.042	1.545	1.042	1.548	151.56	151.41	
DHBP-S							
S_0	1.575	1.061	0.996	1.708	145.1	148.1	
S_1	1.669	1.053	1.013	1.671	141.7	150.2	
DHBP-D							
S_0	1.538	1.073	1.538	1.073	144.5	144.5	
S_1	1.674	1.046	1.674	1.046	140.9	140.9	
DHBP-D							
S_0	0.968		0.968				
DHBP+MeOH							
S_0	1.001	1.663	1.008	1.633	148.19	148.67	1.912
S_1	1.067	1.489	1.049	1.518	152.44	151.90	1.902

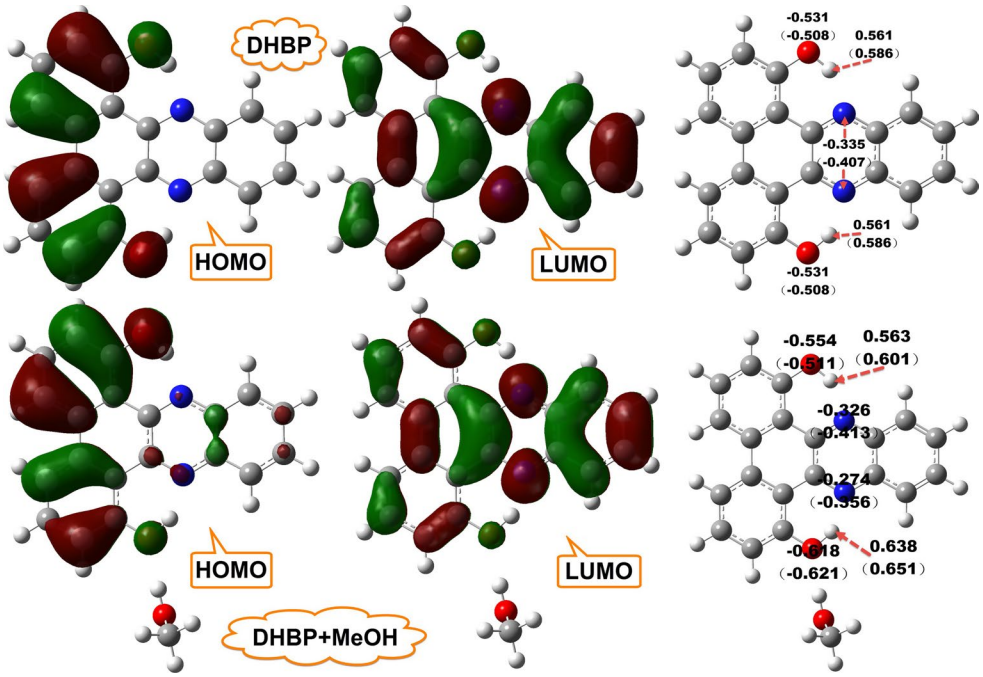

Fig. 2 Frontier molecular orbitals (HOMO and LUMO) of DHBP and DHBP+MeOH; the NBO charges (excited state shown in the *bracket*)

3.2 Frontier molecular orbitals and electronic spectra

The first excited state of DHBP, DHBP-S, DHBP-D, DHBP+MeOH, configuration 1 and 2 are fully optimized by TDDFT/CAM-B3LYP/6-31++G(d,p) based on the ground state optimized geometric conformations. The frontier molecular orbitals (FMOs) [44, 45] can provide essential information of the molecule properties in excited states and the nature of excited-state configuration can be further investigated by charge transfer analysis. According to our calculation, the $S_0 \rightarrow S_1$ transition for DHBP molecule is calculated to be 436 nm with the large oscillator strength of 0.3909, while the $S_0 \rightarrow S_2$ transition is calculated to be 379 nm with the oscillator strength of 0.0001. As for DHBP+MeOH, the photo-excitation is also mainly from S_0 state to S_1 state. Therefore, only the HOMO and LUMO orbitals combined with the NBO charges are presented in Fig. 2. The relative data of configuration 1 and 2 were present in the Supporting Information.

The DHBP molecule clearly shows π character for the highest occupied molecular orbital (HOMO) and π^* character for the lowest unoccupied molecular orbital (LUMO), with a predominant $\pi\pi^*$-type transition from HOMO to LUMO. Much of the current literatures on hydrogen bond indicate that the electron located on the hydrogen bond group, such as O–H group and N atom, can directly influence the intramolecular hydrogen bonds. In DHBP molecule, the electron is mainly located on hydroxyl groups in ground state and on N atoms in first excited state. It can be reasonably deduced that the charge transfer is primarily from electron donor O–H group to the N atoms along the intramolecular hydrogen bond upon photo-excitation. As a result, the intramolecular hydrogen bonds $(O–H\cdots N)_I$ and $(O–H\cdots N)_{II}$ are both strengthened, which may further trigger the proton transfer. The participation of methanol molecule also slightly decreases the electronic density on the hydroxyl group in position II, which means it will inhibit the charge transfer from hydroxyl group to nitrogen atom which caused by photo-excitation. As for configuration 1 and 2, the extension of π-conjugation framework has no visible influence on the characteristic functional group. In addition, the natural bond orbital (NBO) charges can be presented for detailed investigation on the charge redistribution. In configuration 1, the negative charge distributed on the O atom of hydroxyl group decrease from −0.558 (S_0) to −0.525 (S_1) together with that increment on the N atom from −0.280 (S_0) to −0.311 (S_1). The charge on the O atom decrease from −0.519 (S_0) to −0.450 (S_1) and that on the N atom increase from −0.342 (S_0) to −0.399 (S_1) in configuration 2. In BDHP molecule, a similar variation tendency also be found, which both decrease from −0.531 (S_0) to −0.508 (S_1) on the O atoms and increase from −0.335 (S_0) to −0.407 (S_1) on the N atoms. It can be noted that the electron density on N atoms enhanced with the increment of π-conjugation framework in S_1 state. And the increment of electron density on nitrogen atom can enhance the intramolecular hydrogen bond and promote the proton transfer. As for the DHBP+MeOH, the participation of methanol molecule makes some different influence. In position I, the charge on the O atom decrease from −0.554 (S_0) to −0.511 (S_1) and that on the N atom increase from −0.326 (S_0) to −0.413 (S_1). In position II, the charge on the O atom have

Table 2 Stokes shift, electronic absorption and emission energy (nm) calculated by TDDFT/CAM-B3LYP/6-31++G(d,p)

	1-enol	1-keto	2-enol	2-keto	DHBP	DHBP-S	DHBP-D	DHBP + MeOH
Absorption	396		443		436			426
Emission	452	635	517	647	486	522	602	488
Stokes Shift	56	239	74	204	50	86	166	62

slight abnormal increase from −0.618 (S_0) to −0.621 (S_1) and that on the N atom also increase from −0.2740 (S_0) to −0.356 (S_1). It can be deduced that the proton donor methanol molecule can inhibits the excited-state hydrogen bond strengthening in S_1 state.

The Stokes shift, electronic absorption and emission energy were present in Table 2 and the corresponding electronic spectra were present in the Supporting Information. The calculated absorption peak of DHBP is located at 436 nm, which is in good consistent with the experiment data at 429 nm [26]. The calculated normal fluorescence peak is located at 486 nm. The good agreement between the calculated data and experimental results indicates that the calculation method is reliable enough to describe this system. The participation of methanol molecule significantly increases the fluorescence intensity, but barely change the absorption and emission peak position. The fluorescence peaks of DHBP-S and DHBP-D molecule are located at 522 and 602 nm, respectively. In configuration 1, the proton migration creates a large Stokes shift about 239 nm, while that in configuration 2 is decreased to 204 nm. It also can be note that in DHBP molecule, and the single proton transfer only produces a Stokes shift of 86 nm and the double-proton migration make it change to 166 nm. The reasonable prediction can be got that the extension of π-conjugation framework can decrease the Stokes shift created by the proton migration.

3.3 Potential energy surfaces

In order to clearly reveal the excited-state intramolecular proton transfer mechanism, the geometrical structures at both ground and first excited states were optimized with a series of fixed O–H bond lengths. The potential energy surfaces for DHBP molecule are scanned with varying the $(O–H)_I$ and $(O–H)_{II}$ bond lengths from 0.99 to 1.69 Å in steps of 0.1 Å in S_0 state (Fig. 3) and 1.04–1.74 Å in steps of 0.1 Å in S_1 state (Fig. 4). Various methods have been introduced to measure the proton transfer process, among them, the TD-DFT/CAM-B3LYP method is reliable enough to describe the excited-state proton transfer process. The zero-point energy is chosen under the minimum energy of S_0 and S_1 state PESs, respectively. In order to demonstrate the potential energy surface more clear, the energies of the four minimum points are listed in Table 3.

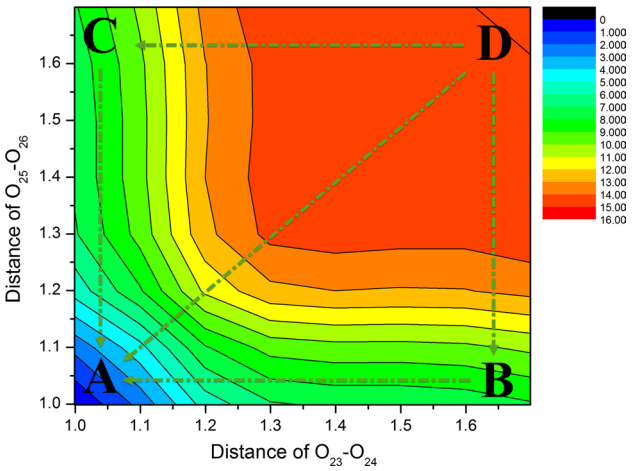

Fig. 3 Isocontour potential energy surface (2D) in ground state for DHBP molecule with fixed O–H distance (Kcal/mol)

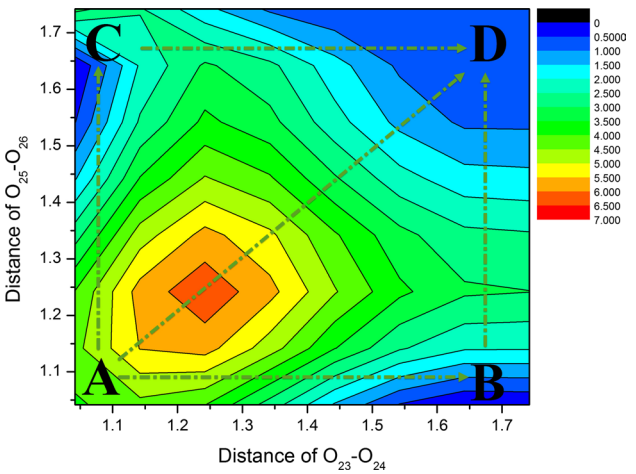

Fig. 4 Isocontour potential energy surface (2D) in first excited state for DHBP molecule with fixed O–H distance (Kcal/mol)

As is shown in Fig. 3, the DHBP (marked as A), DHBP-S (marked as B, C) and DHBP-D (marked as D) are located at the four minima coordinate points. And the relative coordinate points are A (0.99, 0.99 Å), B (1.57, 0.99 Å), C (0.99, 1.57 Å) and D (1.61, 1.61 Å). The relationship of the four minima potential energies can be described as $E_D > E_C = E_B > E_A$. The potential energy barriers in both ground and excited states are also presented in Table 4. The

Table 3 Relative potential energy (Kcal/mol) of the stable configurations in ground and first excited states

	DHBP		DHBP-S		DHBP-D	
	S_0	S_1	S_0	S_1	S_0	S_1
Energy	0	68.78	7.34	64.88	14.43	65.39

Table 4 Potential energy barriers (kcal/mol) among these stable configurations on S_0 and S_1 state PESs

S_0		S_1	
D → A	0.27	A → B or C	0.45
D → B or C	0.18	B or C → D	3.07
B or C → A	0.13	A → D	2.46

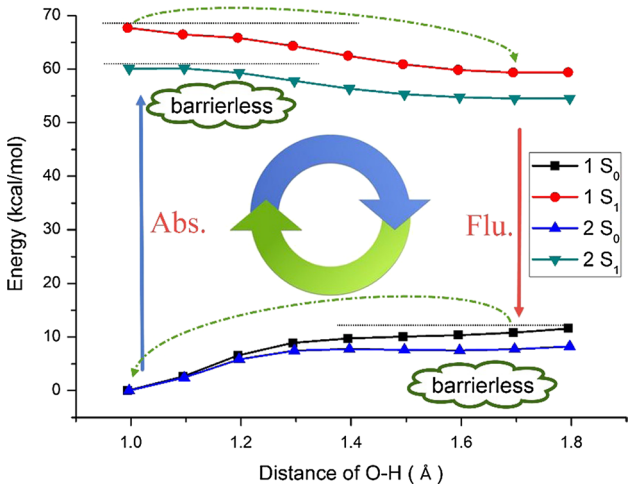

Fig. 5 Potential energy curves of configuration 1 and 2 in both S_0 and S_1 states

proton transfer form point A to point D is an endothermic process with a relative high-energy increase, which means that the proton can not spontaneously transfer from A to D in ground state. The reverse proton transfer potential energy barriers among these points are also calculated and presented: 0.27 kcal/mol separates point D from point A, 0.18 kcal/mol from point D to point B (or C) and 0.13 kcal/mol from point B (or C) to point A. Hence, it could conceivably be concluded that the double reverse proton transfer can spontaneously happened stepwise or concertedly in ground state due to its exothermic process and relative low potential energy barrier.

In first excited-state PES, the coordinates of the four minima points are A (1.04, 1.04 Å), B (1.67, 1.01 Å), C (1.01, 1.67) and D (1.67, 1.67 Å) with the energy relationship $E_A > E_D > E_B = E_C$. The potential energy barrier between point A and point D is 2.46 kcal/mol, while that is 0.45 kcal/mol from point A to point B (or C) and 3.07 kcal/mol from point B (or C) to point D. Moreover, the double-proton transfer process from point A to point D is an exothermic process. Due to the relative low potential energy barrier from point A to point D, the double proton most likely transfer concertedly in S_1 state. In order to investigate the influence of π-conjugation framework on proton transfer process, the potential energy curves of configuration 1 and 2 in both S_0 and S_1 states are scanned with the

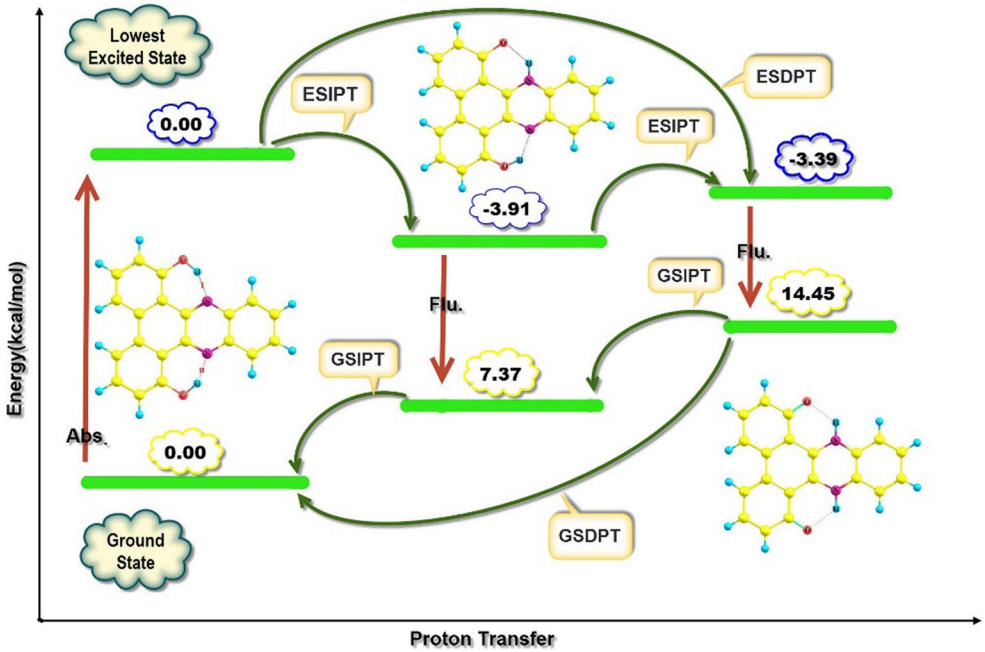

Fig. 6 Excitation and relaxation process

O–H bond length fixed at a series of values. It can be found that with the increment of π-conjugation framework, the energy rise is much lower in configuration 2 in S_0 state (see Fig. 5).

If we take the molecular system as a whole, the excitation and relaxation process can then be summarized and shown in Fig. 6. The ground state DHBP molecule can be photo-excited to the lowest excited state, with low barrier and concertedly (or stepwise) double-proton transfer to form DHBP-D molecule. After the DHBP-D molecule relaxed to the ground state, the reverse double proton can transferred stepwise or concertedly to form DHBP molecule. Taken together, these results provide important insights into the relationship between hydrogen bond and proton transfer, which is the hydrogen bond strengthening after photo-excitation can promote the proton transfer effectively.

4 Conclusion

In the present work, the configuration 1,2,1,8-Dihydroxydibenzo [a,c]phenazine (DHBP) and its isomers are fully optimized by DFT method in ground state and TD-DFT method in first excited state in toluene with IEFPCM. The bond and angle analyses indicate the intramolecular hydrogen bond strengthening phenomenon after photo-excitation. It also found that the increment of π-conjugation framework can visibly enhance the intramolecular hydrogen bond. The IR spectra analysis of hydroxyl group can further prove the conclusion we got. Moreover, the frontier molecular orbitals and NBO charges are presented and discussed in detail. It is found that the electron is mainly transferred from hydroxyl group to pyridine-type nitrogen atom along the intramolecular hydrogen bond upon photo-excitation. The extension of π-conjugation framework increases the negative electron located on the nitrogen atom and then promotes the proton transfer. The Stokes shift created by proton migration is decreased with the extension of π-conjugation framework. In the end of this work, the potential energy surfaces of DHBP molecule are scanned with varying O–H bond lengths in both ground and first excited states. It is found that the double-proton transfer may not happened in the ground state due to the whole reaction is endothermic and the DHBP molecule is the most stable configuration. But the reverse double-proton transfer from DHBP-D molecule to DHBP molecule can spontaneously happened stepwise or concertedly due to its exothermic process and relative low potential energy barrier. After photo-excitation, the double-proton transfer is relative easily happened in concertedly or stepwise due to its relative low barrier from DHBP to DHBP-D. The difference between ground and excited states may propose that the strengthening of intramolecular hydrogen bond can promote the proton transfer effectively.

Acknowledgments This work is supported by National Natural Science Foundation of China (Grant No. 11274096), Innovation Scientists and Technicians Troop Construction Projects of Henan Province (Grant No. 124200510013) and Supported by Program for Innovative Research Team (in Science and Technology) in University of Henan Province (Grant No. 13IRTSTHN016), Supported by The High Performance Computing Center of Henan Normal University.

References

1. Ewa H, Tomasz H (2005) Anal Chem 77:1147
2. Arbeloa FL, Prieto JB, Martínez VM, López TA, Arbeloa IL (2004) Chem Phys Chem 5:1762
3. Fent K, Zenker A, Rapp M (2010) Environ Pollut 158:1817
4. Raymo FM (2002) Adv Mater 14:401
5. Findlay NJ, Jochen B, Inigo AR, Benjamin B, Sasikumar A, Wallis DJ, Martin RW, Skabara PJ (2014) Adv Mater 26:7290
6. Zhao J, Chen J, Cui Y, Wang J, Xia L, Dai Y, Song P, Ma F (2015) Phys Chem Chem Phys 17:1142
7. Ma C, Yang Y, Li C, Liu Y (2015) J Phys Chem A 119:12686–12692
8. Zhao J, Chen J, Liu J, Hoffmann MR (2015) Phys Chem Chem Phys 17:11990
9. Piatkevich KD, Hulit J, Subach OM, Wu B, Abdulla A, Segall JE, Verkhusha VV (2010) P Natl Acad Sci USA 107:5369
10. Paul A, William C, Xinghua S, Boxer SG (2007) P Natl Acad Sci USA 104:20189
11. Wille D-CE, Lüttke PDW (1971) Angew Chem Inter Edit 10:803
12. Dellinger B, Kasha M (1976) Chem Phys Lett 38:9
13. Martinez ML, Cooper WC, Chou PT (1992) Chem Phys Lett 193:151
14. Aquino AJA, Plasser F, Barbatti M, Lischka H (2009) Croatica Chemica Acta 82:105–114
15. Kohei A, Shigehiko H, Shigeki K (2011) Phys Chem Chem Phys 13:11118
16. Yang D, Zheng R, Wang Y, Lv J (2015) J Atom Mol Sci 6:197
17. Li D, Liu Y (2015) J Atom Mol Sci 6:146
18. Yang D, Yang Y, Liu Y (2014) J Clus Sci 25:467
19. Li H, Yang Y, Yang D, Liu Y, Sun J (2014) J Phys Org Chem 27:170
20. Li H, Liu Y, Yang Y, Yang D, Sun J (2014) J Photochem Photobio A Chem 291:9
21. Li H, Liu Y, Yang Y, Yang D, Sun J (2014) Spectrochim Acta A 133:818
22. Zhao GJ, Han KL (2008) J Comput Chem 29:2010
23. Zhao GJ, Han KL (2009) J Phys Chem A 113:14329
24. Zhao GJ, Han KL (2008) Biophys J 94:38
25. Zhao GJ, Han KL (2007) J Comput Chem 127:024306
26. Piechowska J, Virkki K, Sadowski B, Lemmetyinen H, Tkachenko NV, Gryko DT (2014) J Phys Chem A 118:144
27. Jesus AJL, Rosado MTS, Igor R, Rui F, Eusébio MES, Redinha JS (2008) J Phys Chem A 112:4669
28. Kolandaivel P, Nirmala V (2004) J Mol Struct 694:33
29. Ayyappan S, Sundaraganesan N, Kurt M, Sertbakan TR, Özduran M (2010) J Raman Spectrosc 41:1379
30. Comas-Vives A, Harvey JN (2011) Eur J Inorg Chem 2011:5025
31. Frisch MJ, Trucks GW, Schlegel HB, Scuseria GE, Robb MA, Cheeseman JR, Scalmani G, Barone V, Mennucci B, Petersson GA, et al (2009) Gaussian 09 (Revision A02). Gaussian Inc. Wallingford

32. Vosko S, Wilk L, Nusair M (1980) Can J Phys 58:1200
33. Becke AD (1997) J Chem Phys 107:8554
34. Kohn W, Becke AD, Parr RG (1996) J Phys Chem 100:12974
35. Lee C, Yang W, Parr RG (1988) Phys Rev B 37:785
36. Kobayashi R, Amos RD (2006) Chem Phys Lett 420:106
37. Yanai T, Tew DP, Handy NC (2004) Chem Phys Lett 393:51
38. Kobayashi R, Amos RD (2006) Chem Phys Lett 424:225
39. Mennucci B, Cancès E, Tomasi J (1997) J Phys Chem B 101:10506
40. Cances E, Mennucci B, Tomasi J (1997) J Chem Phys 107:3032
41. Cammi R, Tomasi J (1995) J Comput Chem 16:1449
42. Treutler O, Ahlrichs R (1995) J Chem Phys 102:346
43. Furche F, Ahlrichs R (2002) J Chem Phys 117:7433
44. Hu JY, Morita T, Magara Y, Aizawa T (2000) Water Res 34:2215
45. Houk KN, Sims J, Duke RE, Strozier RW, George JK (1973) J Am Chem Soc 95:7287–7301